

ENHANCEMENT OF GRID PRIMARY FREQUENCY RESPONSE USING TYPE 3 AND TYPE 4 WECS WITH VIRTUAL INERTIA CONTROL

Kumaravel .S* Bharathidasan. S.G

Department of Electrical and Electronics Engineering, Sri Venkateswara College of Engineering, Sriperumbudur, Tamilnadu, India-602117

Email-id:kumaravel@svce.ac.in; bharathi@svce.ac.in

Abstract: With proliferation of wind energy, the Variable Speed Wind Turbine inertial response is current research interest. This research work, analyzes Virtual Inertia Control (VIC) technique for VSWT to provide active power support during power imbalance due to sudden load change on large interconnected power system. The traditional maximum power point tracking curve has been modified based on frequency deviation for kinetic energy extraction from VSWT in order to improve primary frequency response of the Grid. The simplified DFIG (Type-3) model, PMSM-FRPC (Type-4) model, IG-FRPC (Type-4) model Wind Turbine Generators (WTGs) with VIC has been aggregated and integrated into two area power systems which include hydro and thermal power plants. The performances of above WTGs are compared under VIC control. The MATLAB/SIMULINK has been deployed to carry out simulation. Simulation results depicted a smooth recovery of rotor speed to optimal value, reduced Rate of Change of Frequency (ROCOF) and improved frequency nadir for effective grid support.

Key words: Frequency Response; VSWT; Virtual Inertia Control; DFIG; PMSM; Induction Generator.

1. Introduction

The projected prediction by 2021 of wind power generation amidst renewable energy resources is 800 GW. The global wind turbine installation may cover nearer to 6% of world electricity demand. The real power imbalance causes the grid frequency to deviate from nominal value. A drop below nominal frequency can be attributed to decrease in generation or increase in demand. In India, frequency varies from 48.5- 51.5 Hz. Mitigation of power imbalance is made possible by primary and secondary frequency control. Hence, inertial response is important because it limits the rate of change of frequency and frequency nadir after power imbalance due to sudden load change [1-3].

The system may face critical frequency stability challenges owing to large penetration of large scale wind power generation in to the grid. Wind power plants through fast and flexible control scheme are expected to render frequency regulation [4, 5].The optimal speed tracking for maximum wind energy capture can be achieved by embedding vector control scheme. It has been observed that VSWT under MPPT mode of operation is not able to provide whole primary frequency response [6, 7].Model of VSWT for simulation of power system dynamics and the role of DFIGs for system frequency regulation are analyzed in [8,9].Here, for inertial response, control system includes a supplementary control loop. Compared with fixed speed wind turbines coupled with conventional generators, variable speed wind turbines are capable of releasing kinetic energy considerably [10-12].The inertial support in VSWT can be rendered through two approaches viz. PD based governor-inertia controller or direct increase in active power output for a specific duration[13-18,22,23].In the afore mentioned works, it can be seen that for a specific system and wind speed, control gains are constant which arises the difficulty to find a specific gain of VSWT for several wind speed conditions. Also, during transient period, the control gain change should be in accordance to system composition in order to store or release of kinetic energy. These control approaches cannot realize smooth recovery to operation of MPPT. In [26-28], inertial response capability of DFIG and PMSM are analyzed with optimal power point control strategy for providing rapid inertial response. The major objectives of this research work are stated as follows, (1) Analysis of impact of various wind turbine generators with DFIG, PMSM-FRPC and IG-FRPC with and without VIC function on frequency stability of an interconnected two-area hydro thermal power system after load disturbance. (2)

Implementation of variable MPPT method to PMSG, DFIG and IG based wind turbine. The organization of this paper is as follows. Section 2 discusses simplified models of various wind turbine generators viz DFIG-WT, PMSM-FRPC and IG-FRPC. Virtual inertia control concept has been introduced in section 3. Section 4 explores the utility of the model developed for primary frequency control through MATLAB/SIMULINK. Simulation studies thus validating the effectiveness of method presented.

2. Model of WECS

2.1. Wind Turbine Model

The power extracted from the WTG is a function of wind speed, air density, rotor size and tip speed ratio and pitch angle.

$$P_t = \left\{ \frac{0.5\rho A}{P_{base}} \right\} v^3 C_p(\lambda, \beta) \quad (1)$$

The mechanical torque can be expressed as follows,

$$T_m = P_t / \omega_t \quad (2)$$

The performance coefficient C_p is taken from reference [8]. The optimal power based on MPPT control is

$$P_{opt} = K_{opt} \omega_t^3 \quad (3)$$

Based on 2MW wind turbine parameters, the $c_p(\lambda, \beta)$ vs λ characteristics for various β values have been obtained and are depicted in Figure 1, while Figure 2 shows the power-speed curve. The Table 1 shows the parameters of 2MW wind turbine.

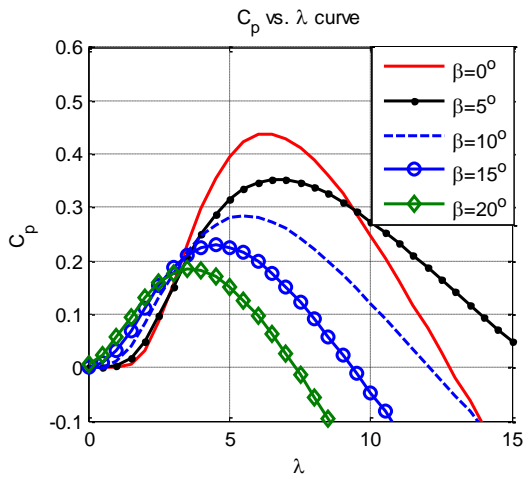


Fig 1. $C_p(\lambda, \beta)$ vs λ

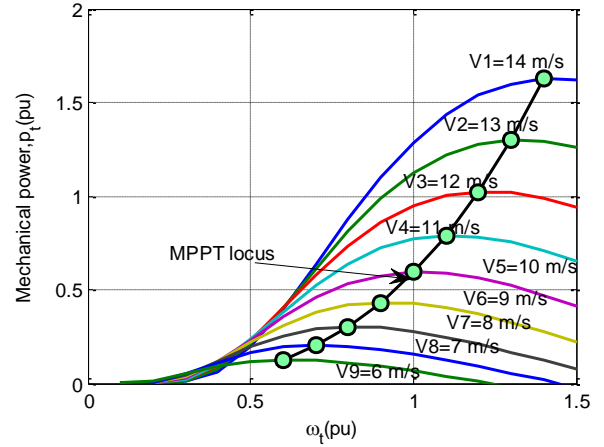


Fig 2. Power –Speed curve

Table 1. Parameters of WT

Parameter	Symbol	Value
Radius of Rotor	R	37.5m
Speed of Rotor	ω_t	9-21rpm
Power rating	P_{base}	2 MW
Wind speed (nominal)	v_{base}	12 m/s
Moment of inertia	J	$5.9 \times 10^6 \text{ Kg m}^2$
Density of Air	ρ	1.225 kg/m^3
Gear box ratio	n	95

2.2. Simplified model of DFIG

The voltage equations in pu for stator and rotor of wound rotor induction machine based on d-q reference frame are as follows [3, 16, 24].

$$v_{ds} = R_s i_{ds} - \Psi_{qs} + \frac{1}{\omega_s} \frac{d\Psi_{ds}}{dt} \quad (4)$$

$$v_{qs} = R_s i_{qs} + \Psi_{ds} + \frac{1}{\omega_s} \frac{d\Psi_{qs}}{dt} \quad (5)$$

$$v_{dr} = R_r i_{dr} - s\Psi_{qr} + \frac{1}{\omega_s} \frac{d\Psi_{dr}}{dt} \quad (6)$$

$$v_{qr} = R_r i_{qr} + s\Psi_{dr} + \frac{1}{\omega_s} \frac{d\Psi_{qr}}{dt} \quad (7)$$

The flux linkages in these equations were referred from [16]. The electromagnetic torque generated is given by following equation

$$\begin{aligned} T_e &= \Psi_{ds} \times i_{qs} - \Psi_{qs} \times i_{ds} \\ &= \Psi_{dr} \times i_{qr} - \Psi_{qr} \times i_{dr} \end{aligned} \quad (8)$$

Through appropriate choice of the reference frame (stator flux oriented vector control), $\Psi_{ds} = 1$ pu, $\Psi_{qs} = 0$, Manipulating equation (4) to (8) the following equations can be obtained.

$$i_{qr} = \frac{1}{R_r} \times \frac{1}{[1+sT_1]} v_{qr} \quad (9)$$

$$T_1 = \frac{L_0}{\omega_s R_r} \text{ and } L_0 = [L_{rr} - \frac{L_m^2}{L_{ss}}] \quad (10)$$

The electromagnetic torque,

$$T_e = i_{qs} = -\frac{L_m}{L_{ss}} i_{qr} \quad (11)$$

The rotor dynamics of WTG is given by

$$\frac{d\omega_t}{dt} = \frac{1}{2H}(T_m - T_e) \quad (12)$$

The simplified model to represent DFIG based on equations (9 -12) is shown in Figure 3 and Table 3.shows the parameters of a 2MW induction machine.

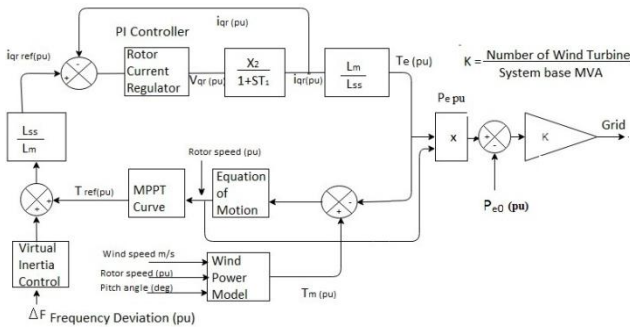


Fig 3. DFIG WTG model

Table 3. Parameters of Induction machine

Parameter	Symbol	Value
Rated power	S_{base}	2MW
Rated frequency	f	50 HZ
Rated Voltage	V	690V
Pole pair	p	2
Generator speed	ω_g	900-2100 rpm
Magnetising Reactance	X_m	3.96545 pu
Stator Reactance	X_{ls}	0.09273 pu
Rotor Reactance	X_{lr}	0.1 pu
Stator Resistance	R_s	0.00491 pu
Rotor Resistance	R_r	0.00552 pu
Inertia Constant	H_{eq}	4.5 sec

The MATLAB/SIMULINK model for DFIG WTG is shown in Figure 4

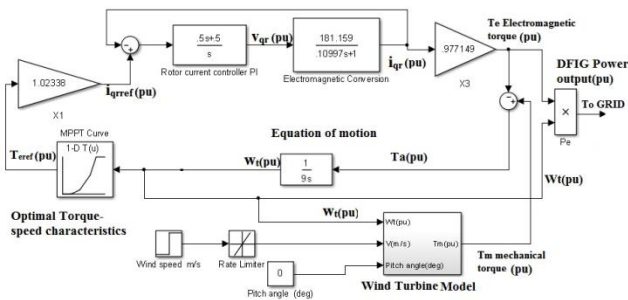


Fig 4. MATLAB/ SIMULINK model for DFIG WTG

2.3. Simplified model of PMSM-FRPC

The voltage equations of PMSM in pu is given by [16, 25].

$$v_{ds} = R_s i_{ds} + \frac{d\Psi_{ds}}{dt} - \omega_g \Psi_{qs} \quad (13)$$

$$v_{qs} = R_s i_{qs} + \frac{d\Psi_{qs}}{dt} + \omega_g \Psi_{ds} + \omega_g \Psi_m \quad (14)$$

The flux linkages in these equations were calculated from,

$$\Psi_{ds} = L_d i_{ds} + \Psi_m \quad (15)$$

$$\Psi_{qs} = L_q i_{qs} \quad (16)$$

The electromagnetic torque is

$$T_e = \Psi_m i_{qs} \quad (17)$$

Manipulating equation (23) to (25) the following equation can be obtained,

$$i_{qs} = \frac{v_{qs} - \omega_g \Psi_m}{R_s + sL_s} \quad (18)$$

The simplified model to represent PMSM based on equation (13) to (18) shown in Figure 5 and 2MVA PMSM parameters are specified in Table 4.

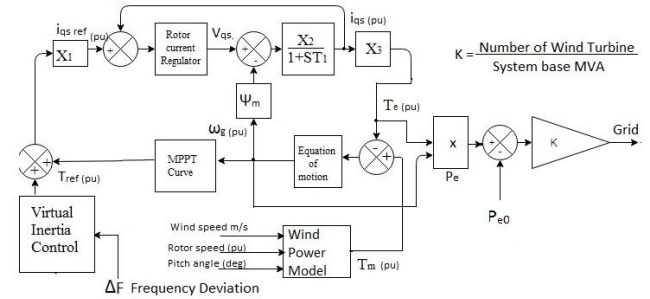


Fig 5. PMSM-WTG model

The MATLAB/SIMULINK model for PMSM-FRPC WTG (Type 4) is shown in Figure 6

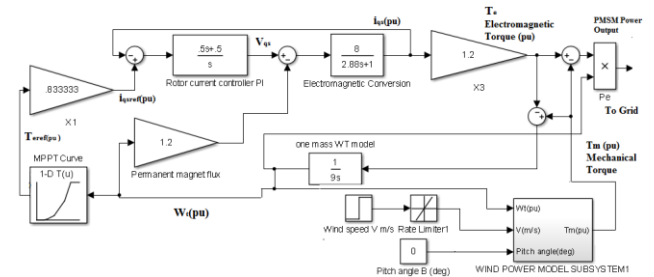


Fig 6. MATLAB/ SIMULINK model for PMSM-WTG

Table 4. Parameters of 2MVA PMSG

Parameter	Symbol	Value
Rated power	S_{base}	2MVA
Frequency	f	50 HZ

Pole pair	p	24
Rotor speed	ω_g	9-21 pm
d-axis Mutual inductance	L_{dm}	0.384pu
q-axis Mutual inductance	L_{qm}	0.344pu
Resistance of Stator	R_s	0.125pu
Leakage Inductance	L_{ls}	0.016pu
Flux of permanent magnet	Ψ_m	1.2pu

2.4. Simplified model of IG-FRPC

Through appropriate choice of the reference frame (vector control) $\Psi_{dr}=1$ pu and, $\Psi_{qr}=0$. Manipulating equations (4) to (8) the following equation can be obtained.

$$i_{qs} = \frac{1}{R_s} \times \frac{1}{[1+sT_1]} v_{qs} \quad (19)$$

$$\text{Where, } T_1 = \frac{L_{ss}}{\omega_s R_s} \quad (20)$$

$$T_e = i_{qr} = -\frac{L_m}{L_{rr}} i_{qs} \quad (21)$$

The simplified model to represent IG-FRPC based on equation (12), (19)-(21) shown in Figure 7 and computed parameters of simplified WTGs model is summarized in Table 5

Table 5. Parameters of simplified WTGs model

WTGs	X1	X2	X3	T1
DFIG	1.02338	181.159	0.977149	0.10997
PMSM	0.8333	8	1.2	2.88
IG	1.025217	203.6659	0.9754	2.6322

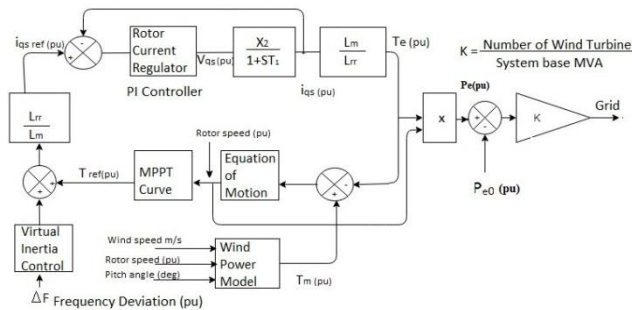


Fig 7 . IG -WTG model

The corresponding MATLAB/SIMULINK model for IG-FRPC WTG (Type 4) is shown in Figure 8.

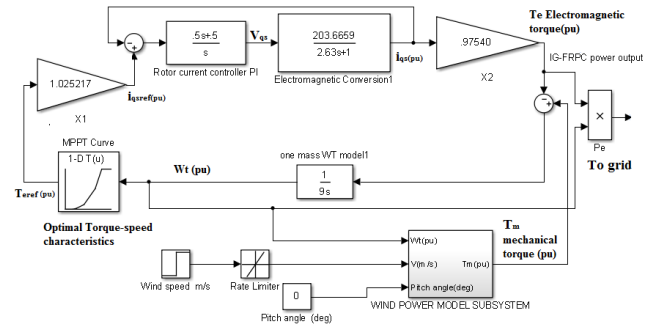


Fig 8. MATLAB/ SIMULINK model for IG- WTG

3. Virtual Inertia Control scheme

In the conventional supplementary control, the torque reference T_{ref} has been modified based on ROCOF and deviation of grid frequency. The additional control signal is given by

$$T_{sp}^* = T_{ref} - K_{df} \frac{d\Delta f}{dt} - K_{pf} \Delta f \quad (22)$$

Where, T_{ref} torque set point based on MPPT curve, T_{sp}^* modified torque reference signal to converter control. The higher values of K_{df} and K_{pf} indicate stronger virtual inertia of VSWTGs. Figure 9, shows the conventional governor inertia controller for VSWT.

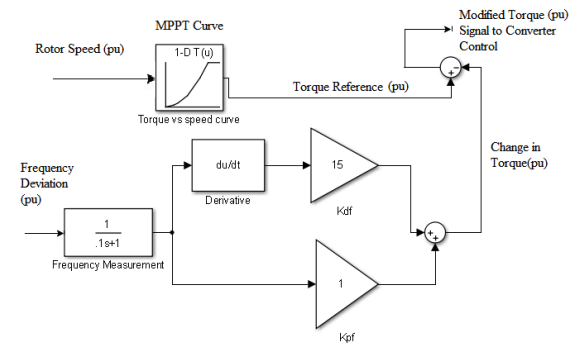


Fig 9. Conventional control for VSWT

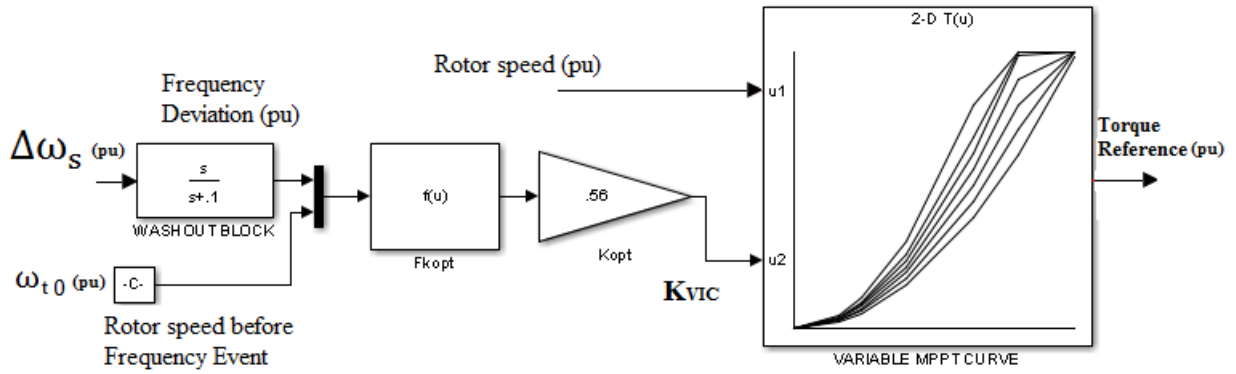


Fig10. Virtual Inertia Control

Based on MPPT control, the rotor speed ω_{t0} and grid frequency deviation Δf are given as the input variable to VIC scheme in order to generate torque reference. The expression to calculate K_{VIC} is given by

$$K_{VIC} = \frac{\omega_{t0}^3}{(\omega_{t0} + \Delta\omega_s K_1)^3} * K_{opt} \quad (23)$$

Where ω_{t0} is the rotor speed before frequency event, K_1 is the coefficient for virtual inertia, $\Delta\omega_s$ is the synchronous grid frequency deviation. Figure 10 shows the VIC based on variable MPPT curve. The optimal power extraction based on MPPT control is represented by equation (24).

$$P_t = \begin{cases} \frac{K_{opt} \omega_0^3}{\omega_0 - \omega_{min}} (\omega_t - \omega_{min}), & \omega_{min} \leq \omega_t < \omega_0 \\ K_{opt} \omega_t^3, & \omega_0 \leq \omega_t < \omega_1 \\ \frac{(P_{max} - K_{opt} \omega_1^3)}{(\omega_{max} - \omega_1)} (\omega_t - \omega_{max}) + P_{max}, & \omega_1 \leq \omega_t < \omega_{max} \\ P_{max}, & \omega_t \geq \omega_{max} \end{cases} \quad (24)$$

In Figure 11, the segment A-B, B-C, C-D represents starting zone ($\omega_{min} \leq \omega_t < \omega_0$), optimizing zone ($\omega_0 \leq \omega_t < \omega_1$) and constant speed zone ($\omega_1 \leq \omega_t < \omega_{max}$) respectively. Figure 12, shows the VIC based variable MPPT curve for three different values of $K_{VICopt} = 0.56$, $K_{VICmax} = 0.9$ and $K_{VICmin} = 0.4$. It is observed that a series of power tracing curves are generated for various K_{VIC} changes from K_{opt} with occurrence of load disturbance in the grid. The torque reference is regulated quickly through switching of operating point A (on MPPT curve) to B (on MPPT left curve) and then to C. The VSWT generator releases the stored kinetic energy through path ABC to support the grid. Post frequency

event, the VSWT must regain its optimal MPPT point.

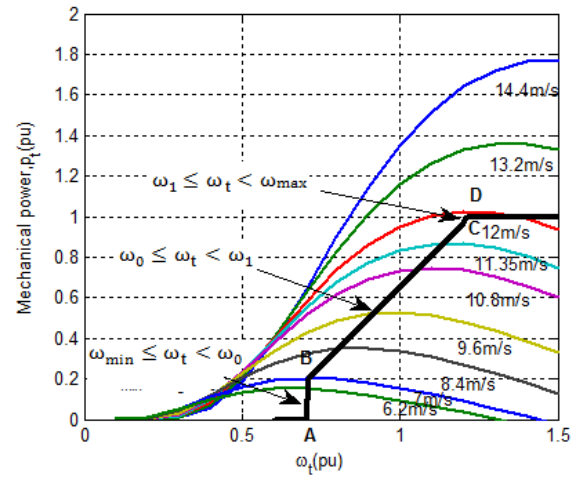


Fig 11. Power-speed curve MPPT control

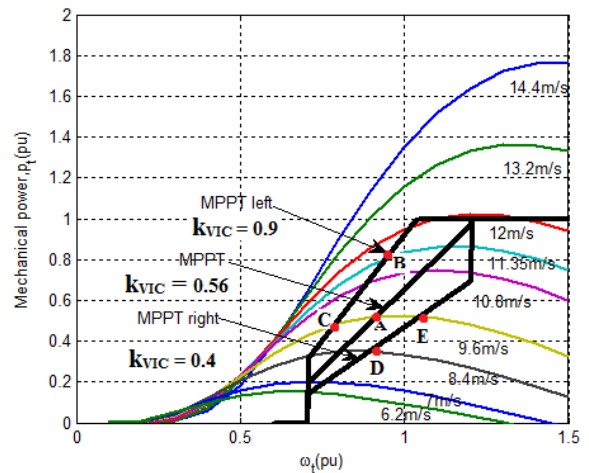


Fig 12. VIC based variable MPPT curve

4. Simulation of aggregated model of wind farm with VIC strategy

To investigate the performance of VIC strategy, a two-area, four machine power system along with aggregated wind farm model housing 270 wind turbines with generators DFIG, PMSM-FRPC and IG-FRPC is established to evaluate the impact of VSWT generators to regulation of system frequency. The two area test system is shown in Figure 13. The system comprises of four 900-MVA conventional generators, and split into two areas.

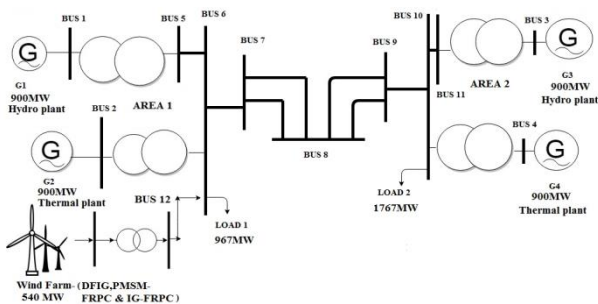


Fig 13. Two area test system

Area1 includes generators G1 and G2. The entire load of 967MW is connected to bus 7. Generators G3 and G4 are in Area2 and Load of 1767MW connected at bus 9 with tie line loading of 400MW. G1 and G3 are treated as hydro plants and G2 and G4 are considered as thermal units.

Wind speed of 12 m/s is assumed. The simplified model for Type 3 and Type 4 WTG model has been incorporated in to the two area power system at bus 12. In these simulations, 2MW type 3 and type 4 designs are combined to yield 540MW wind farm, i.e., Penetration level of 30% (of area 1 capacity) has been simulated for an equal contribution from aggregated model of DFIG, PMSM-FRPC and IG-FRPC WTGs. The various cases of control are as follows,

Case I: VSWTGs without frequency controller (with MPPT control).

Case II: VSWTGs with a conventional df/dt controller.

Case III: VSWTGs with the Virtual Inertia Controller.

Figure 14, shows the MATLAB/SIMULINK sub system model for two area system, aerodynamic

model of wind turbine and different variable speed wind turbine PMSM-FRPC, DFIG and IG-FRPC along with virtual inertia control.

Table 6. Conventional Generating Units Parameters.

Parameter	Symbol	Area ₁		Area ₂	
		G ₁	G ₂	G ₃	G ₄
Plant capacity MVA	P	900	900	900	900
Operating load capacity MW	P ₀	700	700	719	700
Inertia constant	H	6.5	6.5	6.175	6.175
Speed Regulation	R	0.05	0.05	0.05	0.05
Governor time constant(sec)	T _G	0.2	0.2	0.2	0.2
Turbine time constant	T _w /T _{RH}	1	7	1	7
Turbine parameter	R _T / F _{HP}	0.38	0.3	0.38	0.3
Turbine parameter	T _R /T _{CH}	5	0.3	5	0.3
Nominal operating load	P _{d0}	967		1767	
Change in load in pu	ΔP _d	0.11		0	
Frequency Bias	B	41		41	
Equivalent Inertia	H _{eq}	6.5		6.175	
Load Damping	D	1		1	
Change in load in Area 1 MW	ΔP _{d1}	200MW			
Tie line power MW	ΔP _{tie}	400MW			
	a ₁₂	1			

4.1. Dynamic response of two area system with 30% wind farm penetration level

4.1.1. Dynamic Response of two area system

Grid frequency, rotor oscillation of wind turbines and inertial response for a sudden increase in load of 200MW in area1 at 90sec for the three cases of control strategies are evaluated for dynamic response.

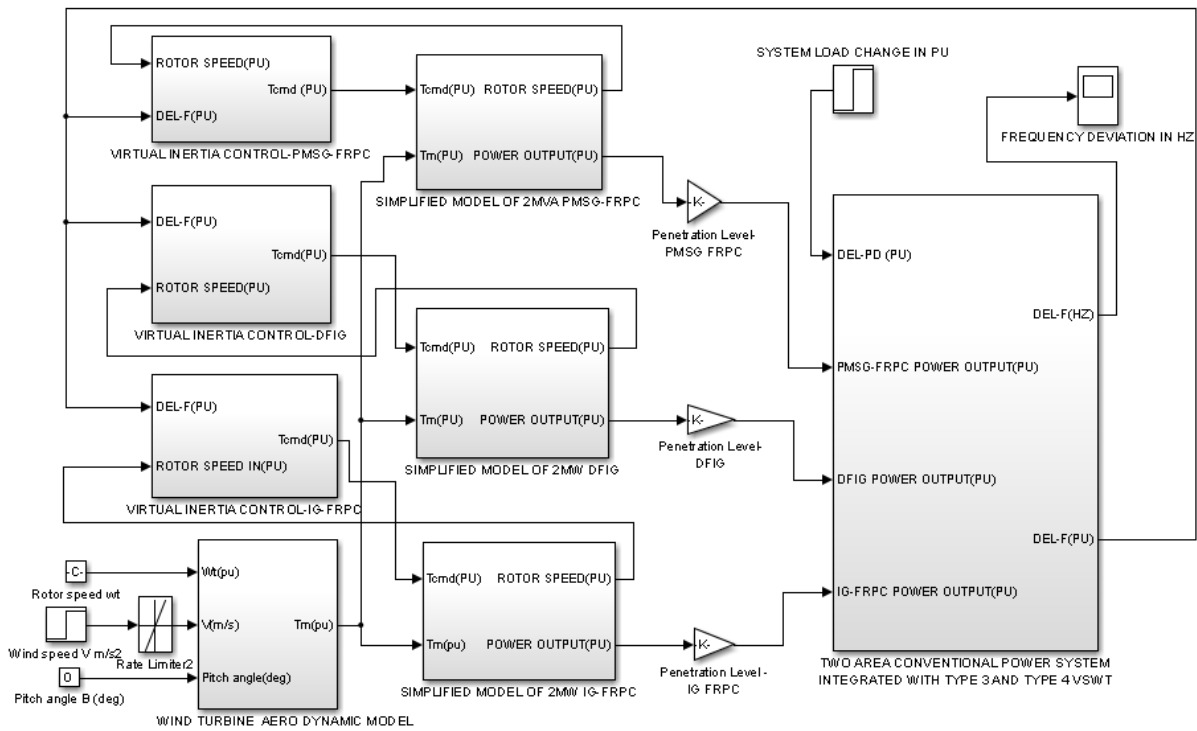


Fig14. MATLAB/SIMULINK model of test system

Without inertial response of the WT, conventional generators bear up the load through governor control. Now, frequency dropped from 50 Hz to 49.47 Hz within 2sec, at a higher ROCOF. With df/dt control loop, frequency drops to 49.55 Hz within 2 sec. With VIC loop, the wind farm increases its output active power rapidly and hence frequency drops to 49.64 Hz within 1.7 sec. It is observed that VIC can increase frequency nadir and reduce the ROCOF. The dynamic rotor speed response with MPPT control, df/dt control and virtual inertia control methods are presented in Figure 16. It is observed that VIC can vary the rotor speed over a wide range to release or absorb more kinetic energy to improve primary frequency regulation. The inertial response for three control strategies viz, MPPT control, df/dt control and virtual inertia control methods are presented in Figure 17. It is evident that VIC can immediately provide active power support of 0.03 pu (54MW) to the grid.

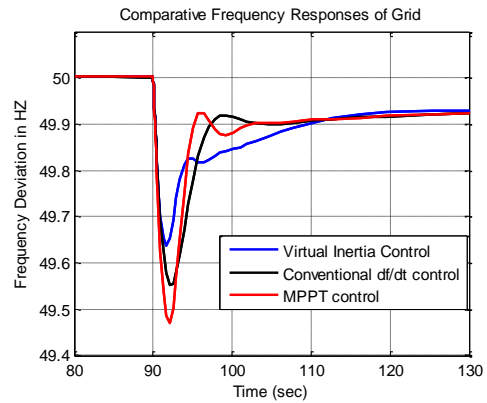


Fig15. Grid Frequency response

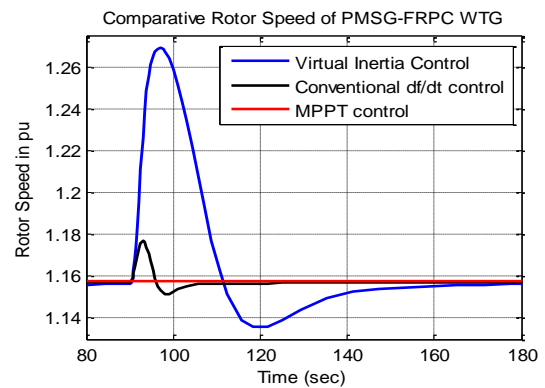


Fig 16.The rotating speed of WTG

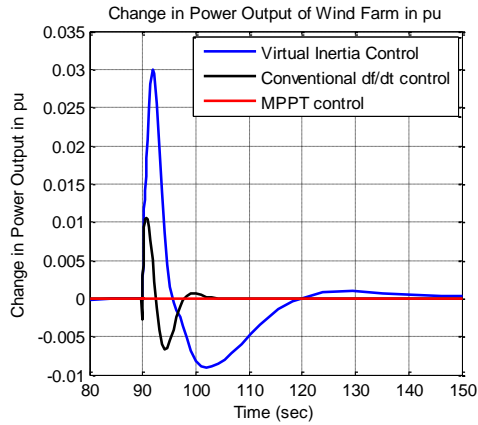


Fig 17. The inertial response of the wind farm

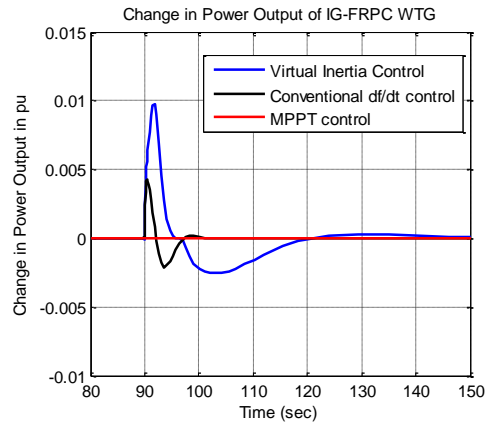


Fig 20. The inertial response of the IG-FRPC WTG

4.1.2. Inertial response characteristics of wind turbine generators

The inertial response of generators under consideration with MPPT control, df/dt control and virtual inertia control methods are presented in Figure (18) to (20), for a sudden increase in load of 200MW in area1 at 90sec

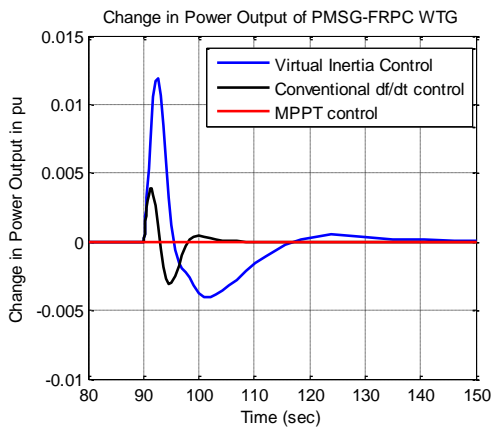


Fig 18. The inertial response of the PMSG-FRPC WTG

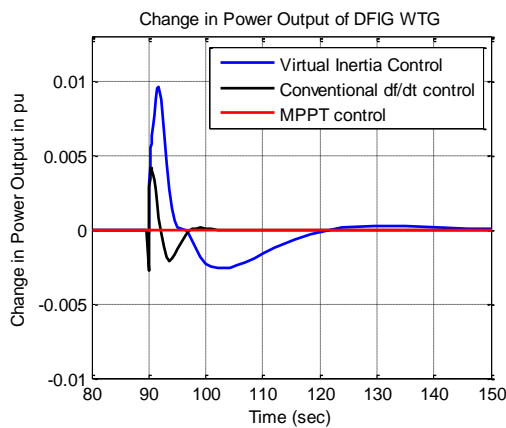


Fig19. The inertial response of the DFIG WTG

The comparisons of inertial responses change in rotor speed and change in electromagnetic torque for different type of WTGs with virtual inertia control methods are summarized in Table 7.

Table 7. Comparisons of PMSG, DFIG and IG WTGs

Comparisons of WTGs with VIC control			
WTGs	Change in power output(pu)	Change in rotor speed(pu)	Change in electromagnetic torque(pu)
PMSM-FRPC	0.0119	0.0708	0.2
DFIG	0.0097	0.0528	0.168
IG-FRPC	0.0097	0.0528	0.1665

It is seen that VIC can change the power output to 0.012pu (21.5 MW), 0.0097pu (17.46 MW) and 0.0097pu (17.46 MW) respectively for initial few seconds. It is observed that, when compared to type 3 DFIG WTG, type 4 PMSG WTG provides strong inertial response and inject more temporary inertial power in to the grid for a short period and the electromagnetic torque for PMSM-FRPC based WTG changes from 0.754 pu to 0.96pu and for IG-FRPC, DFIG based WTGs changes from 0.75 Pu to 0.92pu respectively.

4.2. Dynamic response of two area system with different wind farm penetration level

4.2.1. Dynamic Grid Frequency Response Characteristics

With fast depletion of conventional energy resources, most of the nation's aim to include renewable energy sources (RES) in the grid. The growth extant of inclusion is progressing towards more than 50% of the RES's in to the grid. Hence cognizant of above scenario in this work, the wind penetration levels has been chosen as 10,20,30,40 and up to 50% as shown in Figure 21. At 50% penetration level, extensive decrease in frequency nadir is due to significant rise in wind power penetration. With nadir time remaining in close range, extensive decrease in frequency nadir can be observed. With the inertial support of wind farms at 50% penetration the maximum improvement in frequency nadir can be seen from -0.53Hz to -0.36Hz.

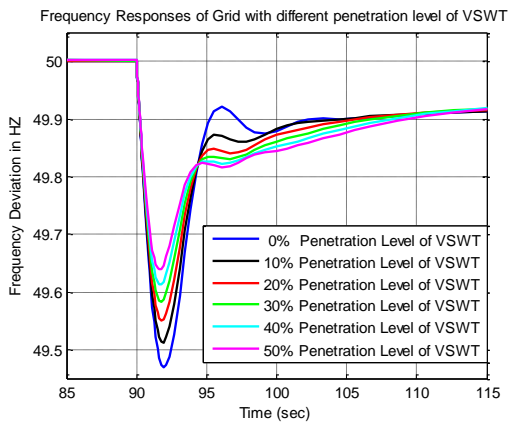


Fig 21. Grid frequency response with different penetration level

Table 8. Comparisons of ROCOF and Frequency nadir for different inertia control methods

Description	ROCOF		Frequency nadir(Hz)		Time to min(sec)	
	30	50	30	50	30	50
MPPT control	0.265	0.265	49.47	49.47	2	2
Conventional Control	0.24	0.224	49.52	49.55	2	2
VIC	0.21	0.18	49.58	49.64	1.7	1.62

4.2.2. Inertial Response Characteristics

The comparative change in power output of wind farm with 30% penetration level and conventional generating units G1, G2, G3 and G4 during sudden increase/decrease in load are presented in Figure 22. It is observed that conventional generation unit power output at steady state is 0.028pu for sudden load increase. The comparative maximum change in power output of conventional synchronous generating units G1, G2, G3 and G4 and wind farm during sudden increase in load are summarized in Table 9.

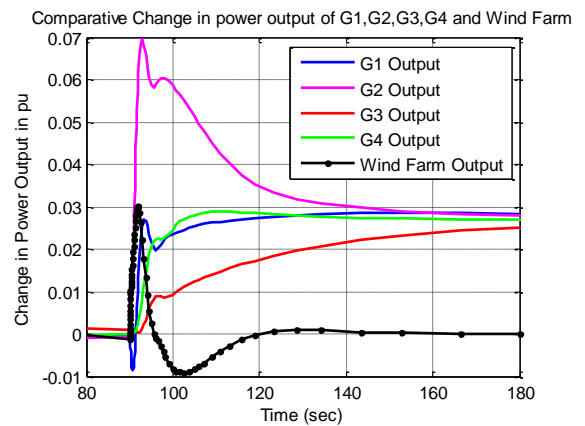


Figure 22. The change in power output With 30% wind farm penetration level

Table 9. Comparisons of inertial response from various generators

Generator or Type	Maximum Change in Power (pu)			Time to Max (sec)		
	0	30	50	0	30	50
Wind penetration Level	0	30	50	0	30	50
G1	0.036	0.0269	0.022	3.9	3.3	3.3
G2	0.090	0.0693	0.059	3.2	2.9	2.9
G3	0.010	0.0089	0.008	6.3	6.6	6.6
G4	0.027	0.0224	0.020	5.7	6.6	6.6
Wind Farm	0	0.03	0.043	0	1.8	1.7

4.3. Dynamic Grid Frequency and Inertial Response Characteristics

Most of the WTs are operated during tropical wind speed conditions, the wind speeds are chosen as 8m/s, 10m/s and 12m/s for the system under study. The comparative change in power output of wind

farm and dynamic grid frequency response for different wind speed conditions are presented in Figure 23 and its summary is given in Table 10. It is seen that high wind speed can increase frequency nadir and reduce the ROCOF and provide more primary frequency support from the wind farm during load disturbance in the grid

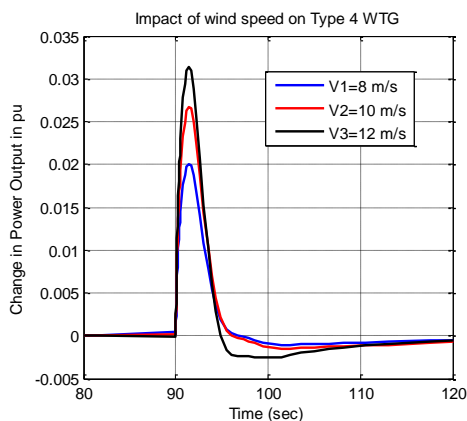


Fig 23. The dynamic response of the change in power output with different wind speed.

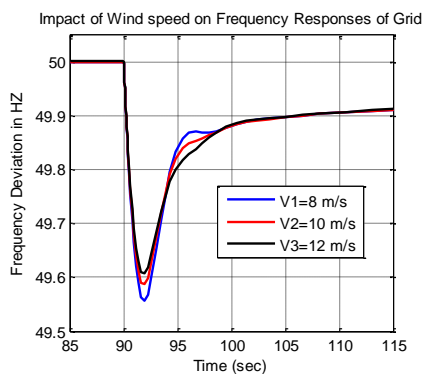


Fig 24 The dynamic response of the grid frequency with different wind speed.

Table 10. Comparisons Inertial response and Frequency Nadir for different wind speed

Wind speed (m/s)	Maximum Change in Wind farm Power Output (pu)	Time to Max (sec)	Frequency nadir	Time to Min (sec)
8	0.02009	1.37	49.56	1.95
10	0.02674	1.37	49.59	1.95
12	0.03139	1.37	49.61	1.95

5. Conclusions

This paper dealt with Inertial Response Analysis of Wind Energy Conversion Systems with Virtual Inertia Control for enhancing primary frequency response of the Grid. The WTG models have been derived. Simplified model of DFIG and PMSG-FRPC, IG-FRPC WTGs and the corresponding MATLAB/SIMULINK model for 2MW WTG has been developed. Frequency sensitive based Virtual Inertia Controller has been designed to provide inertial response. Simulation of aggregated model of wind farm on the two area power system incorporating three control strategies has been carried out resulting in the dynamic response characteristic with 30% penetration level of Wind Farm and inertial and grid frequency response characteristics for various penetration levels and wind speeds respectively.

It can be concluded that, that a smooth recovery of rotor speed to optimal value has been obtained. With Virtual Inertia Control, reduced rate of change of frequency (ROCOF) and improved frequency nadir are achieved for effective grid support. It has been noted that the dynamic frequency response of PMSG-FRPC WTG is nearly same as that of DFIG based WTG. However, PMSG WTG is capable of providing stronger inertial response over DFIG WTG.

References

1. World Wind Energy Association, Available online: <https://library.wwindea.org/2019/02/18/global-statistics-2018-preliminary/> (accessed on 07 April 2019).
2. Central Electricity Authority, Available online: http://www.cea.nic.in/reports/monthly/installed_capacity/2019/installed_capacity-02.pdf, (accessed on 07 April 2019).
3. Kundur P.: *Power System Stability and Control*, 1st ed. McGraw-Hill, New York, USA, 1994; p.581–626.
4. Nordic Grid Code (Nordic Collection of Rules), Nordel, Tech. Rep., 2007, p.74-78.
5. Technical Requirements for the Connection of Generation stations to the Hydro-Québec Transmission System, Hydro-Québec, Tech. Rep., 2019, 59-66.

6. Pena, J., Clare, C.; Asher G. M.; *DFIG using back-to-back PWM converters and its application to VSWE*, IEE Proc. Electr. power Appl, 1996, 143,231–241.
7. Muller, S.,Deicke, M., De Doncker R. W.: *DFIG systems for wind turbines*, IEEE Industrial Application Magazine.,2002, 8, 26–33.
8. Sloatweg, J. G.: *General model for representing VSWTs in power system dynamics simulations*, IEEE Transaction on Power Systems.,2003, 18, 144–151.
9. Ekanayake, J.B., Holdsworth, L., Jenkins N.: *Comparison of 5th order and 3rd order machine models for DFIG wind turbines*, Electric Power Systems Research, 2003, 67 ,207-215.
10. Ekanayake, J., Jenkins, N.: *Comparison of the response of DFIG and FSIG wind turbines to changes in network frequency*, IEEE Trans. Energy Conversion.,2004, 19,800–802.
11. Lalor, G., Mullane, A., Malley, M. O.: *Frequency control and wind turbine technologies*, IEEE Transactions on power systems, 2005, 20, 1905-1913.
12. Mullane, A., Malley, M. O.: *The Inertial Response of Induction-Machine-Based Wind Turbines*, IEEE Transactions on Power Systems, 2005, 20, 1496-1503.
13. Morren, J.,Haan, S., Kling, W. L., Ferreira, J. A.: *Wind turbines emulating inertia and supporting primary frequency control*, IEEE Transactions on Power System.,2006, 21,433–434.
14. Ramtharan, G.; Ekanayake, J. B.; Jenkins, N.; *Frequency support from DFIG wind turbines*, *IET Renew. Power Generation*, 2007, 1, 3–9.
15. Almeida de, R.G., Lope,s J.A.P.: *Participation of DFIGs in system frequency regulation*, IEEE Trans. Power Systems., 2007, 22,944–950.
16. Ekanayake J.B., Jenkins N. Strbac G.: *Frequency Response From Wind Turbines*, Wind Engineering, 2008, 32,6, 573–586.
17. Ullah, N.R., Karlsson, D. Thiringer, T.,: *Temporary primary frequency control support by VSWTs—potential and application*, IEEE Trans. Power Systems., 2008, 23,601–612.
18. Mauricio, J. M., Marano, A., Gomez-Exposito, A., Martinez Ramos J. L.: *Frequency regulation contribution through VSWECS*. IEEE Transactions on Power Systems, 2009, 24, 173-180.
19. Anaya-Lara, O., Jenkins, N, Ekanayake, J.B.,Cartwright, P, Hughes, M.: *Wind Energy Generation: Modeling and Control*, 1st ed, Wiley ,New York, USA.:, 2009, 217-237.
20. Krishnan, R.: *Permanent Magnet Synchronous and Brushless DC Motor Drives*, 1st ed, Taylor and Francis Group, New York, USA, 2010, 279-328.
21. Clark, K., Miller, N. W , S´anchez-Gasca J. J.: *Modeling of GE wind turbine-generators for grid studies*, Gen. Electr. Int., Inc., Schenectady, NY, USA, 2010, 4,1-92.
22. Moore Ian, F.: *Inertial Response from Wind Turbines*, PhD Thesis, Cardiff University, Wales, UK, 2012.
23. Hansen, A. D., Altin, M., Margaris, I. D., Iov, F.,Tarnowski, G. C.: *Analysis of the short-term overproduction capability of VSWTs*, Renewable Energy, 2014, 68, 326-336.
24. Ravichandran, S., Kumudini Devi, R.P.,Bharathidasan,S.G., Evangelin Jeba,V.: *Coordinated controller design of grid connected DFIG based wind turbine using response surface methodology and NSGA II*, Elsevier, Sustainable Energy Technologies and Assessments,2014,8, 120-130
25. Bharathidasan, S.G., Kumudini Devi, R.P., Ravichandran,S.: *Coordinated controller design of PMSG-based wind turbine using response surface methodology and NSGAIL*, International Transactions on Electrical Energy Systems ,2015, 2781-2799
26. Wang, Y., Meng J., Zhang, X, Xu, L.: *Control of PMSG based wind turbines for system inertial response and power oscillation damping*, IEEE Trans. Sustain. Energy, 2015, 6, 565–574.
27. Licari, J, Ekanayake,J,: *Coordinated inertia response from permanent magnet synchronous generator (PMSG) based wind farms*, Journal of the National Science Foundation of Sri Lanka , 2015,43.347-355.
28. Ochoa, D., Martinez S.: *Fast Frequency Response Provided by DFIG Wind Turbines and its Impact on the Grid*, IEEE Trans. Power Syst.,2017, 32, 4002–4011.
29. Krause, P., Wasynczuk, O., Sudhoff, S.: *Analysis of Electric Machinery and Drive Systems*, 2nd ed, Wiley-IEEE Press, New York, 2002,141-190.
30. MATLAB 7.10.0, The Math Works Inc, Natick, MA, USA, 2010.